_____

_____

AN INTRODUCTION TO SUPERHYDROPHOBICITY

Neil J. Shirtcliffe[#], Glen McHale, Shaun Atherton and Michael I. Newton

School of Science and Technology, Nottingham Trent University,
Clifton Lane, Nottingham NG11 8NS, UK

This paper is derived from a training session prepared for COST P21. It is intended as an introduction to superhydrophobicity to scientists who may not work in this area of physics or to students. Superhydrophobicity is an effect where roughness and hydrophobicity combine to generate unusually hydrophobic surfaces, causing water to bounce and roll off as if it were mercury and is used by plants and animals to repel water, stay clean and sometimes even to breathe underwater. The effect is also known as The Lotus Effect[®] and Ultrahydrophobicity. In this paper we introduce many of the theories used, some of the methods used to generate surfaces and then describe some of the implications of the effect.

Keywords
Superhydrophobic; rough; Lotus effect; ultrahydrophobic; textured

---

[#] Corresponding author: Neil. J. Shirtcliffe; neil.shirtcliffe@ntu.ac.uk; Contact: glen.mchale@ntu.ac.uk

Contents

1. Basics of superhydrophobicity
1.1. Interfacial tensions between solids, liquids and gases

To understand superhydrophobicity we begin by considering the surface of a liquid. At the surface, molecules of a liquid have fewer neighbours than those in the bulk. The resulting difference in interaction energy manifests itself as surface tension, γ_{LV}; a force that acts to reduce the surface area of a free liquid. Traditionally, surface tension can be regarded as a force per unit length and is given in units of N m^{-1} or as energy per unit area J m^{-2} [1]. When a volume of liquid can freely adjust its shape, it does so to minimize its surface free energy and since the shape with the smallest surface area is a sphere, a droplet of a liquid tends towards this shape. However, most water droplets we see in nature do not exist as spherical shapes. Larger droplets and droplets that touch surfaces are distorted by gravity and by the interaction between the water and the solid.

By considering dimensional arguments for the force due to surface tension and that from gravity, we can see that surface tension can become dominant at small sizes. Surface tension forces scale as a function of length, R, whereas gravitational forces scale with the mass of the drop, which depends upon a length cubed, R^3, and the density of the liquid, ρ. The ratio of gravitational to surface tension forces for a droplet scales as $\rho g R^3 / \gamma_{LV} R \sim R^2$ (where g=9.81 m s^{-2} is the acceleration due to gravity), and so is large when the length scale is large, but vanishes as the length scale becomes small. This means that the dominant force crosses over from being gravity to surface tension as the characteristic size in a system reduces. If we plot these two lines for water on Earth as in Figure 1 they cross at a size of 2.73 mm, which is called the capillary length for water, $\kappa^{-1} = (\gamma_{LV}/\rho g)^{1/2}$. For drops much smaller than this, as a simple rule an order of magnitude smaller (i.e. <0.273 mm), surface tension dominates. The cross-over from gravity to surface tension dominated behaviour can be seen in a simple paper-clip experiment. A large metal paper-clip lowered carefully onto the surface of water breaks the "skin" and sinks, whereas a small paper-clip remains resting on the surface of the water[1]; it does not truly float, but appears to do due to the "skin effect" of water caused by surface tension. In the natural world, insects are of a size that surface tension is the dominant force. It is, therefore, hardly surprising that, in a world full of ponds and streams, many insects (and spiders) have natural morphological adaptations that enable them to either break through the surface of water or to rest and move on its surface [2, 3]. Some insects walk and skate on water and others can carry a film of air underwater that acts as an artificial gill (known as a "plastron").
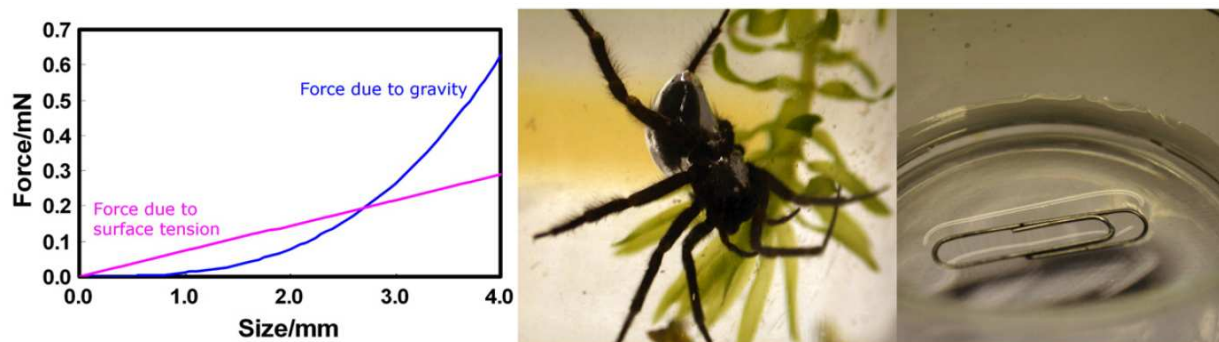

Figure 1. Effects of surface tension. Surface tension plotted against gravity for water on Earth: A water spider *Argyroneta aquatica* with an air film on it and a paperclip suspended on water.

[1] For a video of the paperclip experiment see: http://www.naturesraincoats.com/Introduction.html

1.1.1. Interactions with surfaces

Surface tension, γ_{LV}, relates to the existence of an interface between a liquid and a vapour and is only one example of an interfacial tension. When a droplet of water rests on a solid, two further interfaces, the solid-liquid and solid-vapour, become relevant and also provide interfacial tensions γ_{SL} and γ_{SV}. The balance between these three interfacial forces determines whether a droplet resting on a solid will eventually be pulled out into a film or whether it will remain as a droplet and, if so, the extent of its footprint on the solid surface. On a smooth and flat surface the interaction energy per unit area for a dry surface is γ_{SV}, but for the same surface coated in a thin layer of a liquid there are two interfaces with a combined interaction energy per unit area of $\gamma_{SL} + \gamma_{SV}$. The condition for film formation on a smooth and flat surface is therefore that the energy is lowered [4, 5], i.e.

$$S = \gamma_{SL} + \gamma_{LV} - \gamma_{SV} > 0 \qquad (1)$$

where S has been defined as the spreading power. When the surface is complex in shape, such as at a join between fibres, droplets will be drawn into non-spherical shapes as they try to minimize their total surface free energy by varying the relative areas of the three interfaces, whilst maintaining their volume [6]. The size of droplet will determine to what extent gravitational energy is also a controlling factor. For example, a small droplet of water resting on a horizontal surface will adopt a shape close to a spherical cap, whereas a larger droplet will be flattened into a puddle by gravity.

When a film is not formed and a droplet remains on a surface in a partial wetting state, there is an equilibrium contact angle, θ_e, at the edge of the droplet. This is the tangent angle of the liquid-vapour interface at the three-phase (solid-liquid-vapour) contact line (Figure 2). The contact angle is independent of droplet size and is described by the Young equation [1],

$$\cos\theta_e = \frac{(\gamma_{SV} - \gamma_{SL})}{\gamma_{LV}} \qquad (2)$$

This concept of a single equilibrium contact angle is an idealized view and does not take into account contact angle hysteresis and how the droplet arrived at its resting state through advancing or receding on the surface. For smooth and flat surfaces and water the lowest possible contact angle is 0º (although this can correspond with many values of S) and the highest possible angle is probably less than 120º and is found on fluoropolymers, such as PTFE (Teflon®).
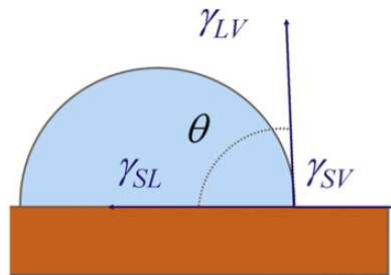
Figure 2. Diagram showing the forces at the three-phase contact line of a liquid droplet on a solid.

1.1.2. Superhydrophobicity of leaves

The leaves of the sacred Lotus are unusual in that water rolls off them in balls with contact angles much greater than that on flat PTFE. As droplets roll away they gather and transport dust and leave the surface of the leaves clean; this has become known as the Lotus effect® [7, 8]. Highly mobile droplets of water on leaves with a contact angle in excess of 150º appear to be quite common in the plant world, example crop plants including the cabbage family (*brassica*), garden peas (*Pisum sativum*) and Taro (*Colocasia esculenta*) and ornamentals including Hosta (*Hosta*), Lady's Mantle (*Alchemellia*) and Lupin (*Lupinus*) (Figure 3).

Figure 3. Nasturtium, Ladies mantle and Lupin leaves with water droplets on them.

The leaves achieve this effect by creating a surface that is both rough and hydrophobic. The roughness enhances the effect of the surface chemistry to produce the superhydrophobicity. Because the waxes plants use to create superhydrophobicity are quite oleophilic, the contact angle to oils is quite low. In this case, the roughened waxes increase the interaction of the oil with the surface and cause the leaves to be self poisoning, i.e. oils spread on them better (wider in extent and faster) than they do on equivalent flat surfaces.

1.2. Hydrophobicity, hydrophilicity and superhydrophobicity

A completely hydrophilic (or wetting) surface is one on which a film forms so that eq. (1) is valid and for $S=0$, eq. (2) shows the threshold for this corresponds to $\theta_e=0°$. A completely hydrophobic surface would be one for which it was energetically unfavourable for a droplet to have any contact whatsoever and this corresponds to $\theta_e=180°$. All droplets that have finite contact angles between these two values are therefore partially wetting. The change in sign of eq. (2) can be used to separate the intrinsic behaviour of a surface for a given liquid. If $\gamma_{SV}<\gamma_{SL}$, the contact angle will be less than 90º and the surface is conventionally described as hydrophilic, whereas, if $\gamma_{SV}>\gamma_{SL}$, the contact angle will be greater than 90º and the surface is conventionally described as hydrophobic. It could be argued that if a droplet attaches to a surface there is a level of absolute hydrophilicity (or absolute hydrophobicity) and larger contact angles, including those above 90°, simply indicate relatively less hydrophilicity of the surface [9, 10]. As there is always an attraction between a solid and a liquid, due to van der Waals interactions, all surfaces would be hydrophilic under this interpretation. The opposite terminology, where all surfaces with non-zero contact angles with water are considered hydrophobic has also been used and signifies $\gamma_{LV}=\gamma_{SV}-\gamma_{SL}$ from Eq. (2) which means it is the threshold above which it is energetically unfavourable to make the surface completely wet (i.e. replace the vapour interface by a liquid one). The $\gamma_{SV}=\gamma_{SL}$ threshold (contact angle 90°) remains useful as it is the threshold where capillaries with uniform cross-section along their lengths fill, is significant for slightly rough surfaces as will be shown shortly and some important properties depend upon the cosine of the contact angle, which also changes sign at 90°. At this point, as $\gamma_{SV}=\gamma_{SL}$, there is no change in energy on wetting the surface (it is the threshold where putting a solid into a liquid without changing the liquid air interface goes from releasing energy to costing energy) so the liquid forms a shape to minimize the liquid vapour area, i.e. a half sphere.

Surfaces with hydrophobic tendencies can be enhanced to superhydrophobicity by the addition of roughness or, more accurately, a certain type of topography. This can be viewed as a physical amplification of the chemistry of the surface [11]. It can increase the contact angle well beyond that possible by chemistry alone and can approach 180° in some cases. It can also decrease the contact angle towards 0° more than might be expected from the chemistry along. The amplification effects of surface topography can be understood in the same manner as in deriving the Young equation.

1.3. Young's equation, force balance and surface free energy arguments

One way of looking at the Young equation is that it represents a force balance at the contact line between the three interfaces (solid-liquid-vapour). In a two-dimensional model the horizontal components of the interfacial forces have magnitudes γ_{SV}, γ_{SL} and $\gamma_{LV}\cos\theta$, where θ is the instantaneous (dynamic) contact angle. The balance of interfacial forces at the contact line is γ_{SV}-γ_{SL}-$\gamma_{LV}\cos\theta$. In equilibrium, the contact line is static and this force must vanish so that,

$$\gamma_{SL} + \gamma_{LV}\cos\theta_e = \gamma_{SV} \tag{3}$$

and this leads directly to Young's equation, (equation 2).

This approach works well with a flat surface, but is less easy to understand when considering a rough surface which has sharp spikes on which resolving forces and angles is less obvious. In the 2D model in figure 3 the contact line advancing and receding over the surface would take on different local contact angles as it advanced around the curves of the roughness and the surface could have points at which a slope is multi-valued [12, 13].

An alternative approach that inherently involves averaging over a small area is to consider surface free energy changes for perturbations of the contact line (Figure 4) [4]. As the contact line advances along the surface by a small distance, ΔA, it replaces the solid-vapour interface by a solid-liquid one, thus causing a change in surface free energy of $(\gamma_{SL}$-$\gamma_{SV})\Delta A$. However, the liquid-vapour interface also gains in length by an amount $\gamma_{LV}\cos\theta$, where we have assumed that any change in the contact angle is a second order effect. The total change in surface free energy, ΔF, accompanying an advance of the contact line is therefore,

$$\Delta F = (\gamma_{SL} - \gamma_{SV})\Delta A + \gamma_{LV}\cos\theta\Delta A \tag{4}$$

Since local equilibrium corresponds to the minimum of surface free energy with a zero gradient, the change in free energy for a small movement of the contact line will necessarily be zero. Thus, we can set ΔF to zero and on rearranging the equation we recover the original Young's equation.
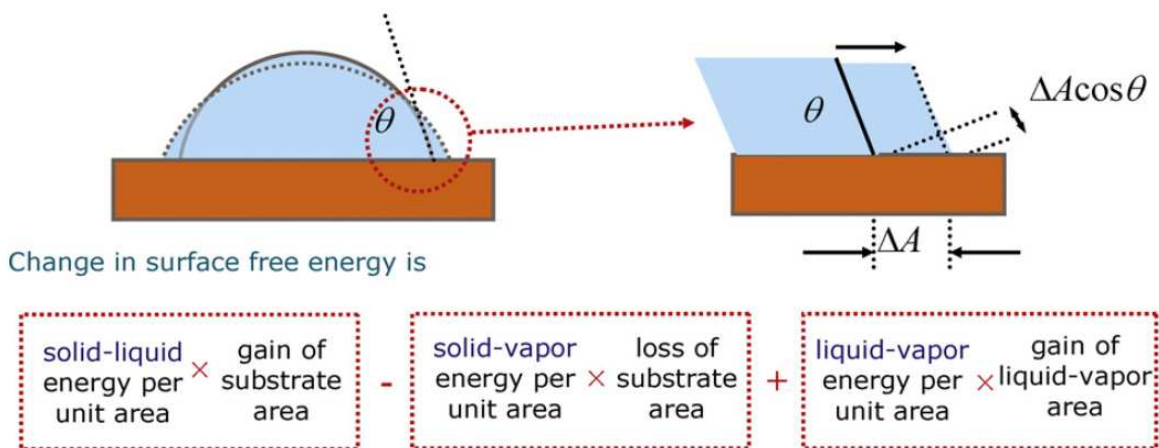
Figure 4. Contact angle and surface free energy.

The surface free energy argument is a simple one that relies on a contact line being able to freely explore changes in the energy landscape by making infinitesimal advances and retreats from its existing position. It therefore assumes vanishing contact angle hysteresis and it only guarantees a local equilibrium based upon the surface properties of the area in the vicinity of the local contact

line; areas deep within the droplet contact area or well outside of it are irrelevant [14, 15]. As presented, the argument describes a 2-dimensional model rather than the 3-dimensional world. However, provided axial symmetry is maintained the argument can be applied to any radial segment. If extended to 3 dimensions a surface free energy argument can also be applied to local contact line changes of drops of complex shapes on complex surfaces.

1.3.1 Rough surfaces and surface free energy arguments

There are two extreme cases that can occur at a rough, hydrophobic surface when a water droplet is applied. One possibility is that the droplet could maintain contact with the entirety of the rough surface (the Wenzel case), thus increasing the interfacial contact area (Figure 5) [16, 17]. Alternatively, the droplet could skip between the peaks of the roughness (the Cassie case), thus leaving a patchwork of solid-liquid and liquid-vapour interfaces below it [18, 19, 20].
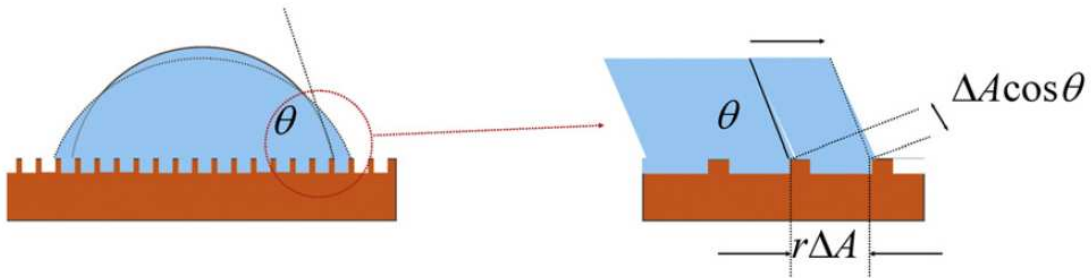

Figure 5. Contact angle on rough surface using Wenzel equation.

The surface energy argument can be used again in both cases. In the Wenzel case, the surface areas of both the solid-liquid and the solid-vapour interfaces associated with the advance of the contact line are increased by a factor r, the specific surface area of the rough surface at the contact line (how many times more surface there is than if it were flat). This leads to a surface free energy change,

$$\Delta F = (\gamma_{SL} - \gamma_{SV})r\Delta A + \gamma_{LV} \cos\theta\Delta A \qquad (5)$$

which for local equilibrium, ΔF=0, gives,

$$\cos\theta_W = \frac{r(\gamma_{SV} - \gamma_{SL})}{\gamma_{LV}} \qquad (6)$$

This can be substituted with Young's equation, equation 2, to give,

$$\cos\theta_W = r\cos\theta_e \qquad (7)$$

This is known as the Wenzel equation, as it was first formulated by Wenzel [16]. In Wenzel's equation, the roughness factor, r, acts as an amplification of the effect of the surface chemistry determined term, $\cos\theta_e$; small changes in θ_e become larger changes in θ_W, provided complete contact is retained between the liquid and the solid. The importance of θ_e=90° is the changeover in sign of the cosine term. When θ_e<90°, the effect of increasing roughness r is to further reduce the Wenzel contact angle towards 0°, but when θ_e>90°, the effect of increasing roughness is to further increase the Wenzel contact angle towards 180°. Thus, Wenzel roughness emphasizes the intrinsic tendency of a surface towards either complete wetting or complete non-wetting [11].

An alternative possibility is that as roughness increases, the liquid no longer retains complete contact with the solid at all points below the droplet. In this other extreme, the liquid bridges between surface features and no longer penetrates between the spaces separating them; a simplified

example using flat-topped surface features is shown in Figure 6. In this simple example we are assuming that the liquid only contacts the flat parts of the surface and that the meniscus below the drop is flat, implying that the gaps between the features are much smaller than the curvature of the meniscus due to the liquid's weight and the pressure exerted by the top meniscus.
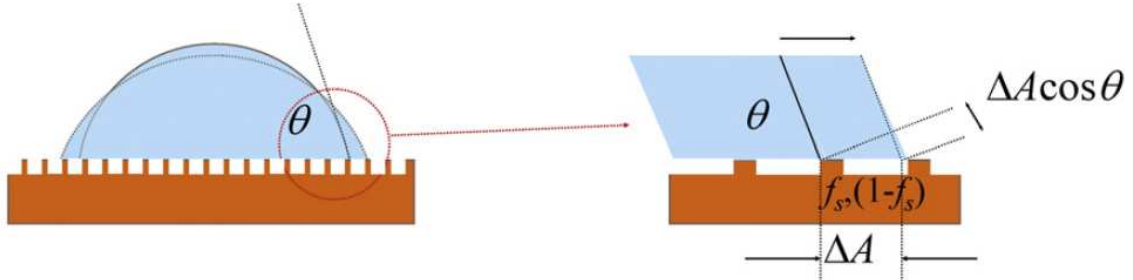

Figure 6. Contact angle on rough surface using Cassie-Baxter formula.

As the contact line advances by ΔA, only a fraction $f_s \Delta A$ of the solid is contacted by the liquid and the remainder $(1-f_s)\Delta A$ is then the area bridged between surface features; this remainder involves the creation of a liquid-vapour interface. The surface free energy change is then,

$$\Delta F = (\gamma_{SL} - \gamma_{SV})f_s \Delta A + (1 - f_s)\Delta A \gamma_{LV} + \gamma_{LV}\cos\theta\Delta A \tag{8}$$

At equilibrium this can be simplified to,

$$\cos\theta_{CB} = \frac{f_s(\gamma_{SV} - \gamma_{SL})}{\gamma_{LV}} - (1 - f_s) \tag{9}$$

or, using equation 2,

$$\cos\theta_{CB} = f_s \cos\theta_e - (1 - f_s) \tag{10}$$

Equation 10 is known as the Cassie-Baxter formula, or Cassie and Baxter's formula [18]. In contrast to the Wenzel case, small changes in θ_e became smaller changes in θ_{CB} although the absolute value of θ_{CB} is larger than θ_e. Whilst the surface is topographically structured, and one may even say it is rough, the roughness factor, r, does not directly enter into the Cassie-Baxter formula. Indirectly roughness does matter because the balance between roughness and solid surface fraction determines the threshold Young's equation contact angle at which the Cassie-Baxter state becomes the more energetically stable compared to the Wenzel state; a point examined in detail by Bico *et al.* [21].

The Cassie-Baxter equation (equation 10) can also be viewed as a weighted mean (by interfacial fraction at the contact line) of the Young's equation contact angle and a contact angle against the vapour (180° and so cos180°=-1). This way of thinking also reveals that if the pores in the surface are prefilled with the liquid the contact angle there will be 0° and the central negative sign will change to positive, indicating a reduction in observed contact angle [22]. This alternative case is not superhydrophobicity, but can occur on otherwise superhydrophobic surfaces with the right (or wrong) preparation.

1.4 How the suspended state stays suspended

The Cassie and Baxter state with the liquid only wetting the tops of the surface structure can seem strange and this often leads to the use of the terminology "air trapping"; a misleading terminology because the lack of liquid penetration is not a consequence of an inability of air to escape. A useful analogy is that of a bed of nails (a *Fakir's carpet* [23]), where if someone sat on a single upturned nail they would receive a puncture wound, but if they lie carefully across many nails close together their weight is spread across a reasonable area and the local pressure at any one nail is not sufficient to cause injury.[2] In no way is the air beneath trapped and it does not help support the person at all. Indeed in Figure 7 we can see that small objects (apples) thrown against a bed of nails are impaled, but that a larger object (a person) is not even when they are also supporting the weight of a second person. Whilst this is only an analogy, the idea of skin effect due to surface tension and the existence of a natural length scale for objects to be able to bridge asperities are useful in considering superhydrophobic surfaces. Whether a liquid penetrates or not is determined by the cost in surface free energy for wetting down the surface structure [23, 24, 25, 26].
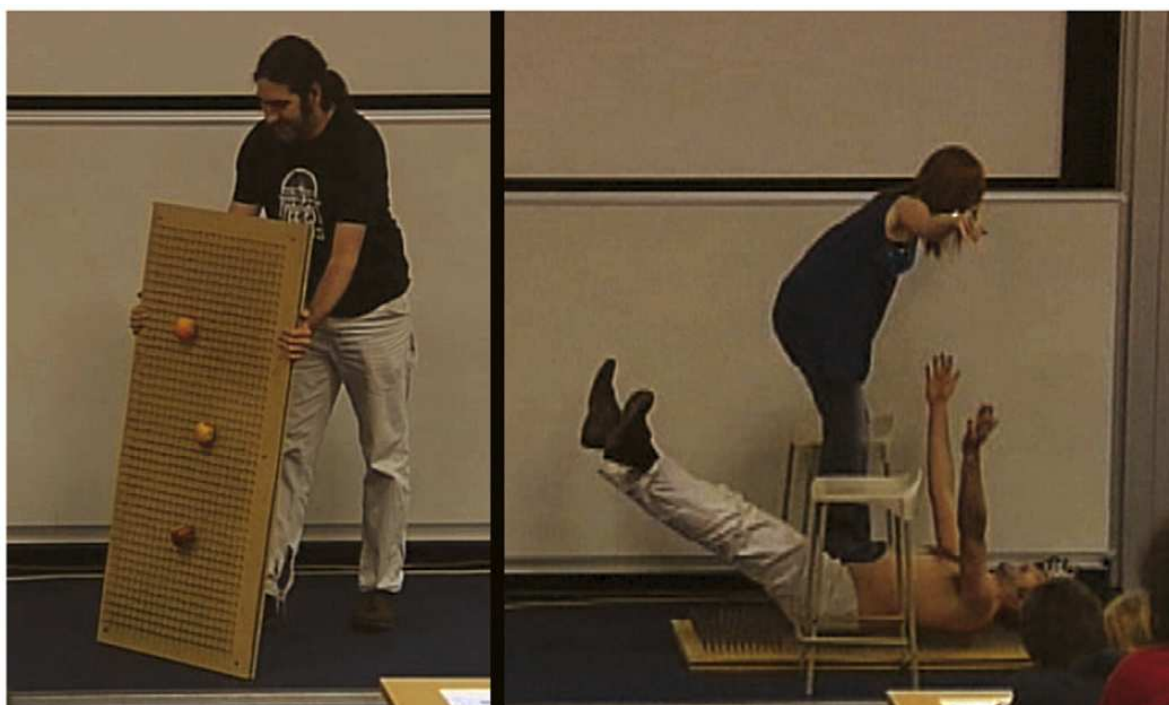
Figure 7. Dr James Hind and Laurice Fretwell (NTU) demonstrating a bed of nails.

1.5. Important considerations when using Wenzel and Cassie-Baxter equations

As with all equations it is important to remember how these equations were derived when using them.

Using Young's equation introduces the assumption that we are investigating equilibrium contact angles. This is important, because in practice the Young angle relates to an idealized concept of a contact angle that is not always observable, particularly on roughened or heterogeneous surfaces because the contact line can become locally pinned on sharp points or local heterogeneities.

Whilst the spacing of features below the entirety of the droplet determines whether

---

[2] For a video of a person on a bed-of-nails see: http://www.naturesraincoats.com/Introduction.html

penetration into the surface structure occurs, it is the spacing and feature shape at the contact line that determines the observed contact angle. Moreover, the predicted Cassie-Baxter (or Wenzel) contact angle assumes a change in ΔA that samples the contact line over a length that is completely characteristic of the surface. For a completely random surface structure, this may be reasonable on average around the entirety of the contact line. However, when the surface has a characteristic symmetry in its surface features or their arrangement on the surface this assumption becomes less certain. One suggested criteria is that if axial symmetry is observed, then these equations will be reasonable approximations [15]. This would not be the case if the surface structure had strong symmetry, such as in the form of parallel grooves. In this situation, the contact angle would be different parallel and perpendicular to the grooves and the droplet would become distorted from an axially symmetric shape. Similarly, if the scale of the roughness is too great the contact line will become locally distorted and an average contact angle will be difficult to measure.

The use of small changes in the contact line to calculate the local equilibrium state has significant implications. In particular, it means that parts of the surface inside or outside a small region close to the contact line do not affect the local equilibrium state. It also means that large scale variations in the surface, including roughness, can only be considered locally. As an example, if the surface consists of two concentric regions concentrically with the outer area having a lower Young's equation contact angle and a droplet of suitable volume is placed centred in the middle, there will be two stable contact angles dependent upon the wetted area at the initial deposition. The first is one with the droplet fully on the inner region with the contact angle of the inner region. The second is with the droplet fully on the outer region, but with the lower contact angle. This can be seen in the figure 8. In this situation, it would be incorrect to use the Cassie-Baxter equation because for either state, small changes of the contact line of the droplet only sample one type of surface.
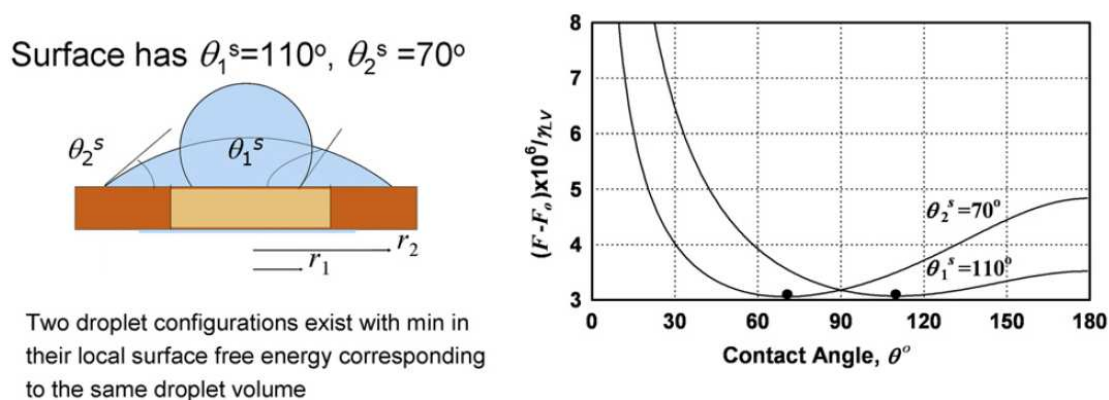

Figure 8. Multiple stable contact angles for concentric surfaces. Reproduced with permission from McHale [15]. Copyright American Chemical Society 2007.

Similarly, if the regions are made thinner and packed in a concentric series it is still not possible to use an average of the two surface as the contact line will always be wholly on one surface or the other provided the droplet remains centred on the structure. In the limit the drop will always be on a hydrophilic region but projecting over a hydrophobic region, allowing it to assume any angle between the values of the hydrophobic and the hydrophilic regions. The consideration of surface free energy change that was used to calculate both Wenzel's and Cassie and Baxter's equations requires that an average of the pattern is sampled by the (approximately circular) contact line. Implicit in this is the requirement of a randomly mixed surface with a small feature size or of changes by the liquid on the surface that average out preferred directions due to any symmetry in the surface pattern (Figure 9).
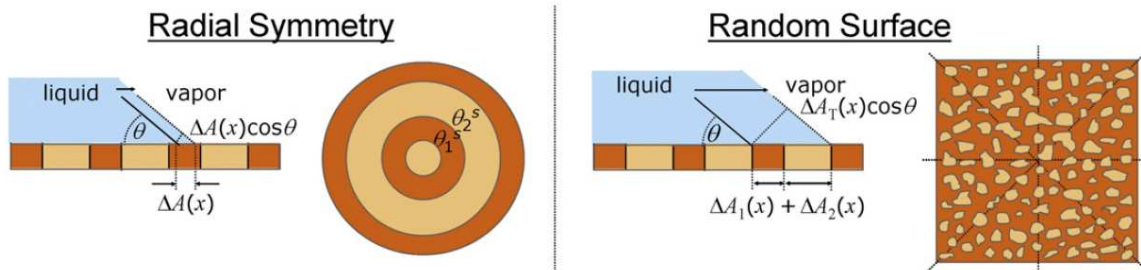
Figure 9. Concentric surface and random surface, only the random surface will follow Cassie and Baxter's equation. Reproduced with permission from McHale [15]. Copyright American Chemical Society 2007.

If the surface pattern beneath the contact line varies with location it is not possible to use global averages of roughness or solid surface fraction in equation 7 and equation 10 although values local to the contact line may be used. In terms of wetting, the roughness and solid surface fraction properties are not one's of the surface itself, but of the surface sampled locally by the contact line of the liquid. This variation in pattern with position can be used to produce a pattern of surface wettability with variation of the local contact angle from one side of a droplet to the other and so create a driving force to direct the motion of a droplet [11, 27, 28, 29]. Whether motion occurs depends on droplet size and the contact angle hysteresis. This situation is shown in Figure 10.
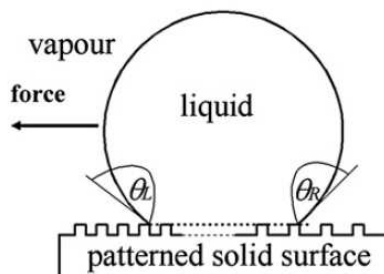

Figure 10. A patterned surface with changing pattern, giving rise to a lateral force on a drop placed on it. Reproduced with permission from McHale *et al.* [27].

This can be realised in various ways, a fractal copper surface was used in one of our studies [27], causing water to move in a chosen direction.

1.6. More complex topography

Often the structure of a naturally occurring surface is more complex than the models of simple flat-topped surface protrusions. In these cases, it is often difficult to measure the roughness factor r and/or the solid surface fraction f_s, that a droplet experiences. It is also possible that neither a pure Wenzel nor a pure Cassie state will occur. Some of the roughness can be wetted and some can be bridged and the balance between these two can change with the type of liquid.

One approach to dealing with this is to consider each level of roughness as consecutive transformations of the droplet-surface system. For example, for pillars possessing rough tops there are several possibilities, two of which are shown in figure 11. In the first case, the small scale structure at the top of pillars is in a Wenzel state, but the large scale structure is in a Cassie state. Mathematically, the Young's equation contact angle, θ_e, for the surface is first transformed using the Wenzel equation and the roughness factor for the small scale structure, r_{small}, to get a Wenzel contact angle, $\theta_W(r_{small}, \theta_e)$. Subsequently, this Wenzel contact angle is transformed using the Cassie-Baxter equation with a solid-surface fraction for the larger scale structure, f_s^{large}, to obtain the final contact angle (i.e. $\theta_{CB}(f_s^{large}\theta_W(r_{small}, \theta_e))$) [30]. In the second case in figure 11, the Cassie-Baxter equation is used twice, first with the solid fraction for the small-scale structure and then with the solid fraction for the large-scale structure. This type of approach can be extended to other combinations of surface types.
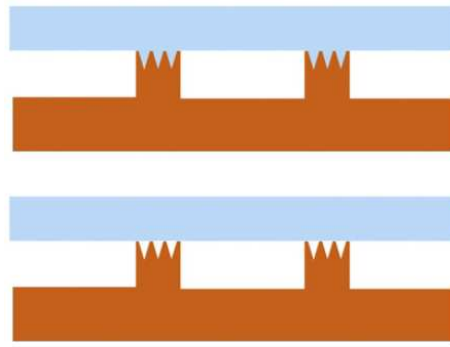
Figure 11. Multiple scales of roughness can be treated separately and still produce a valid contact angle prediction. Liquid filled case: Create Wenzel angle and use in Cassie-Baxter equation. Non-filled case: Create Cassie-Baxter angle for top and use in Cassie-Baxter for large scale structure

A classic example of a combined Wenzel and Cassie-Baxter surface is a set of parallel fibres. In this case, a liquid wet down the sides of the fibre until its local contact angle on the fibre is the same as Young's equation. Whilst the approach used in figure 11 remains valid, the difference is that both the roughness factor, r, and solid surface fraction, f_s, themselves become dependent on the type of liquid (through θ_e). In principle a curved structure, such as a fibre or a "ball-on-a-stick" can suspend a liquid even when its Young's equation contact angle is substantially less than 90°, even down to 0° [31, 32, 30, 31]. This is particularly important in constructing oil repellent surfaces, where surfaces with intrinsic contact angles greater 90° may not exist; the importance of an inward curve to create a re-entrant surface has been emphasized by Tuteja *et al.* [33, 32]. In these cases involving curvature, both the roughness factor r and the solid surface fraction f_s are dependent upon the contact angle, θ_e, as well as the pattern shape as the liquid wets different sections of the curvature depending on the local contact angle (Figure 12). This has consequences for the extent to which droplets on these surfaces can freely move (i.e. "sticky" versus "slippy" surfaces) since although a bridging state is produced it also involves more extensive contact between the liquid and solid at those points where contact is maintained.
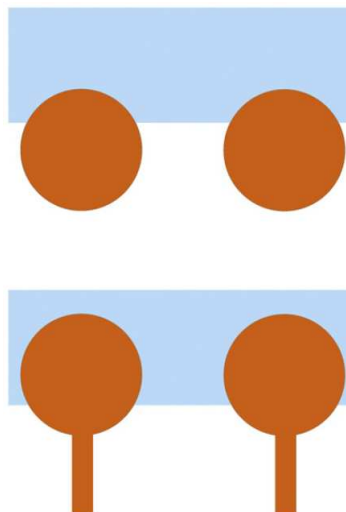
Figure 12. Top: curved pillars require both Cassie-Baxter and Wenzel equations and the factors depend on the contact angle as well as the pattern geometry. Bottom: re-entrant surfaces can support a bridging state for low contact angles.

Complex topography is often more effective at generating high contact angles and low hysteresis than simpler surfaces. It has been shown that multiple overlaid scales of roughness are more effective than the sum of the parts, increasing how easy it is to generate a bridging state, how easy it is to maintain and its effectiveness. This has been shown theoretically [34] and experimentally [35,36], an example is shown in figure 13.
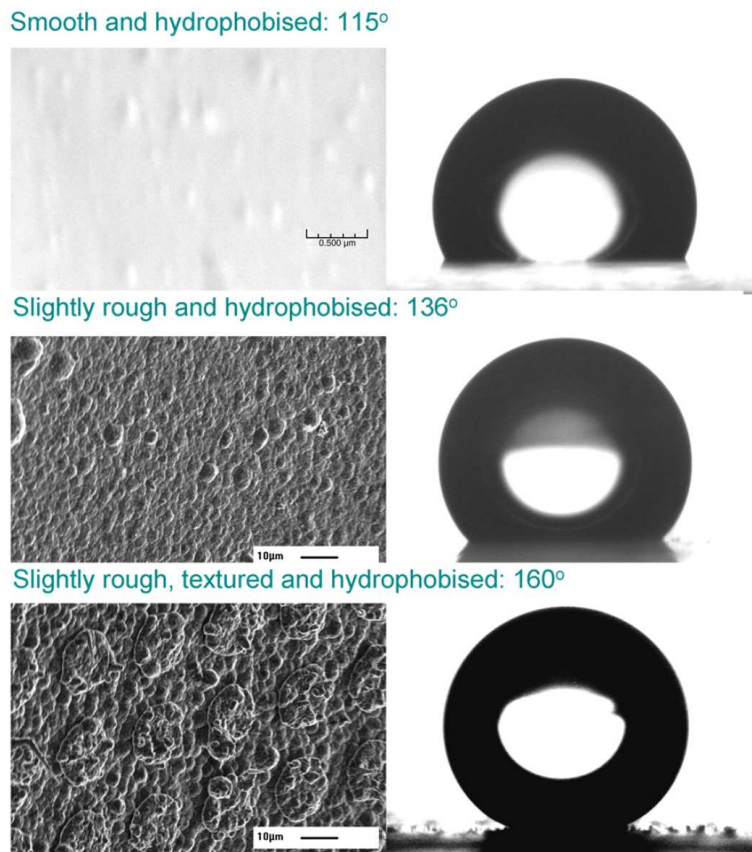
Figure 13. A surface with two levels of roughness can be considerably more hydrophobic than one with one even when each roughness has little effect on its own. Reproduced with permission from Shirtcliffe *et al.* [36]. Copyright Wiley-VCH Verlag GmbH & Co. KGaA 2004.

2. Consequences of superhydrophobicity

2.1. Amplification and attenuation of contact angle changes

If we plot the expected contact angles on a rough surface against those on a smooth surface for different initial contact angles we find that the Cassie-Baxter contact angle changes little as the contact angle of the equivalent flat surface changes, while the Wenzel contact angle does, although it saturates at 0° and 180° [11] (Figure 14).

Figure 14 Contact angles on a rough surface against those on a smooth surface for different initial contact angles for both Wenzel (penetrating) and Cassie-Baxter (bridging) states. Reproduced with permission from G. McHale & M.I. Newton, Colloids and Surfaces **A206** (103) (SI) (2002) 193-201. Copyright Elsevier 2002.

13

This implies that the Wenzel state amplifies the effects of any change in the chemistry of the surface, whilst the Cassie-Baxter state attenuates it. In practise the wetting tends to cross over from fully wetting Wenzel at low contact angles to non-wettin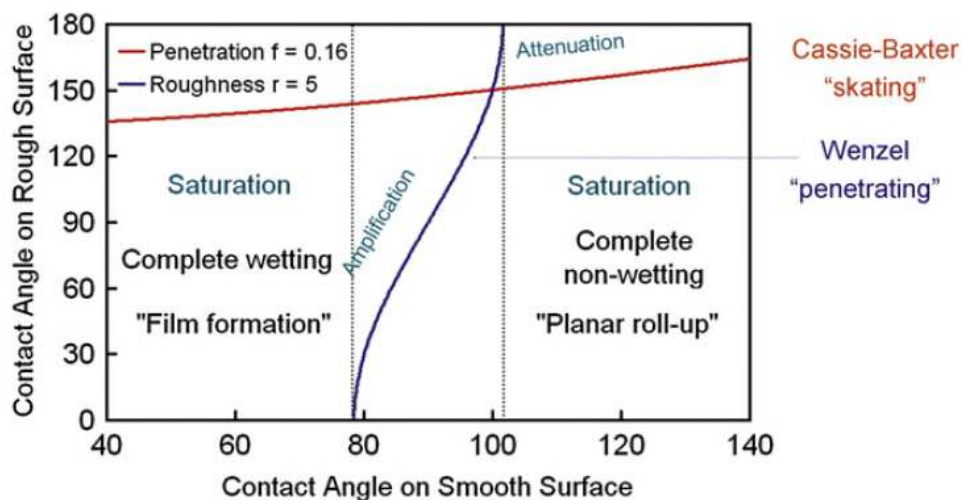g Cassie-Baxter at higher ones [37]. This is shown experimentally in figure 15 [11]. The liquid was changed in this case while keeping the surface constant, but changes in surface chemistry with the same liquid would be equivalent. The response changes through saturation, amplification and attenuation as the wetting state changes from wetting to bridging.
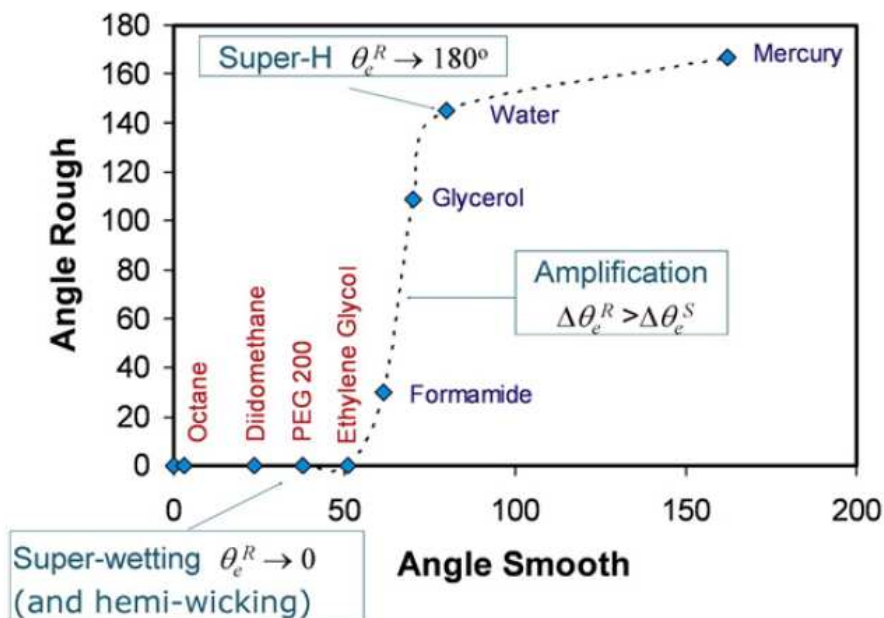

Figure 15. Experimental data showing saturation of Wenzel wetting at low angle (liquids with contact angles on flat below 50° all go to 0° on the rough surface); amplification at medium angles (the difference between formamide and glycerol is around 15° on a flat surface, 55° on the rough one); and attenuation at higher angles (the difference between water and mercury is lower on the rough surface than the flat one). Reproduced with permission from McHale *et al.* [11]. Copyright Royal Society of Chemistry 2004.

Several liquids that have a low contact angle on a flat surface have a zero contact angle on the rough surface. This raises the question of the definition of a superhydrophilic (or superwetting) surface, since roughness is not required to create film-forming surfaces even for water. However, creating a film where one would not otherwise be created could be regarded as super-wetting. Moreover, whilst a rough surface may have many liquids which on it display a non-zero contact angle, this does not make them all equivalent; the rate at which they approach a final state is affected by the flat surface contact angle and the roughness (i.e. superspreading). It has been shown that the rate at which a droplet spreads is different on a textured surface than on a flat one [38].

2.2. Bridging-to-penetrating transition

Some complex undercut (overhanging) topographies, such as the "ball-on-a-stick" or fibres mentioned earlier go into a bridging mode unless the advancing liquid has a low enough contact angle with the surface to get round the cusp of the structure. This idea was discussed by Herminghaus [39].

Another consideration is how far the meniscus bulges down and ripples naturally. This has been considered recently by Tuteja *et al.*, who has defined some characteristic numbers to estimate when a meniscus should touch the bottom of a given pattern [40]. Previous studies have calculated the energy barrier between Wenzel and Cassie-Baxter states [41]. Figure 16 shows how varying the height of a pillar pattern affects the contact angle of a drop of water placed on top [42]. Increasing

height causes an abrupt change from Wenzel wetting to Cassie-Baxter at an aspect ratio slightly below 1 for small drops carefully placed on top. Transition to the Wenzel state can be induced by shaking, allowing the drop to fall from a height or other ways of applying pressure
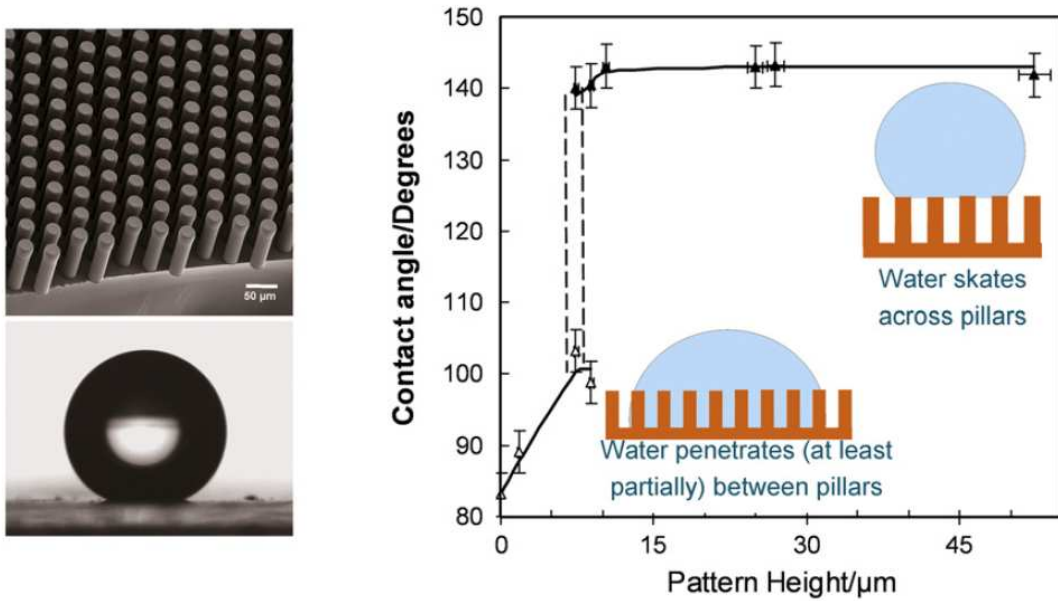

Figure 16. As the height of polymer pillars are increased the contact angle of water drops placed on them increases and then suddenly jumps to a more or less constant value. This is consistent with a change from Wenzel wetting where changes in height will affect *r* to Cassie-Baxter bridging where the distance to the base is irrelevant. Reproduced with permission from Shirtcliffe *et al.* [42]. Copyright Institute of Physics 2004.

As can be seen the changeover is slightly far from sharp. These pillars were evenly spaced round pillars and had diameters of 15 micrometers so the changeover occurs at an aspect ratio slightly below 1.

One simple way to estimate the point at which the Cassie-Baxter bridging state becomes stable is to calculate the contact angles of the wetting Wenzel state and the bridging state and compare them [43].

An example would be the pillars shown in figure 17 (of height *h*). For a given pattern the values of roughness and solid surface fraction for any height *h*, pillar diameter, *D*, and lattice periodicity, *L*, can be calculated for a given equilibrium angle and plotted against each-other.

$$r = 1 + \frac{\pi D h}{L^2}, \quad f_s = \frac{\pi D^2}{4L^2} \qquad (11)$$

The curves in Figure 17 show that for the 15 μm pattern the Cassie-Baxter state will be stable once the height exceeds 21 μm. This is somewhat greater than the values measured experimentally shown in figure 16, but the treatment does not allow for roughness of the sidewalls or projecting edges, which can be seen in the micrograph of the structures and which can contribute to the creation of metastable states.

The other reason that this treatment differs from measured values is that there is an energy barrier between the two states, making one of them stable and the other metastable. On many surfaces this energy barrier is large enough that a drop of water will tend to stay in the state that it is put in (the Cassie-Baxter bridging state for a drop applied from the top) unless forced into the other state. A condensing liquid will always form in contact with the surface so droplets forming this way

15

often begin in the Wenzel state and can be trapped there by the energy barrier in the same way that droplets deposited gently onto the surface will start in the Cassie-Baxter state [44]. The way that water condenses on superhydrophobic materials is of particular interest, because of its potential use in condensers [45, 46]. Surfaces with overhanging structures enhance the energy barrier between the states, making the thermodynamically unstable state kinetically stable.
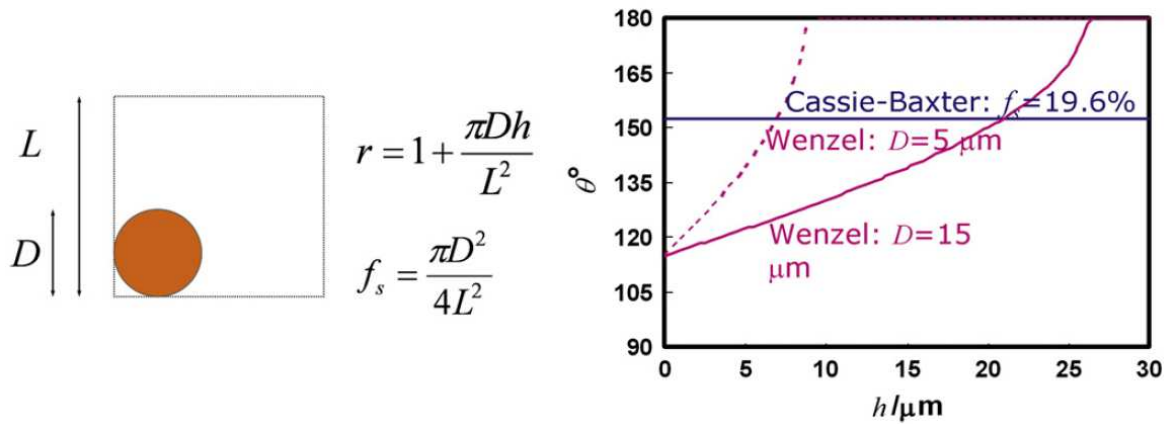

Figure 17. An example of calculated angles for a square array of pillars showing where the two possible configurations are equivalent.

2.3. Contact angle hysteresis

As mentioned at the beginning of this article, one of the characteristics often associated with superhydrophobic surfaces is the tendency for droplets of water to roll or slide on them very easily. This is connected with contact angle hysteresis, which is where a contact interface can take a range of angles without moving. Young's equation suggests that there is only one stable contact angle, but on real surfaces there are a range of stable angles. It is common to observe a droplet of water sitting on a tilted surface with a different contact angle at the front and rear edges. Similarly, if water is steadily added or removed from a droplet, initially the contact line remains static and the contact angle increases or decreases. The highest contact angle before movement is known as the advancing angle and the smallest as the receding angle, defining the range of possible angles. Although an infinitely slow rate of movement is theoretically required to get the real values practical equivalents are relatively easy to measure for low viscosity liquids. These angles can be measured by placing a drop on a surface and varying the volume until the contact line moves or by tilting the substrate until the drop begins to move (Figure 18). There is no theoretical proof that the advancing and receding contact angles measured by these two different methods will be the same, but both give an estimate of contact angle hysteresis and droplet mobility [47].
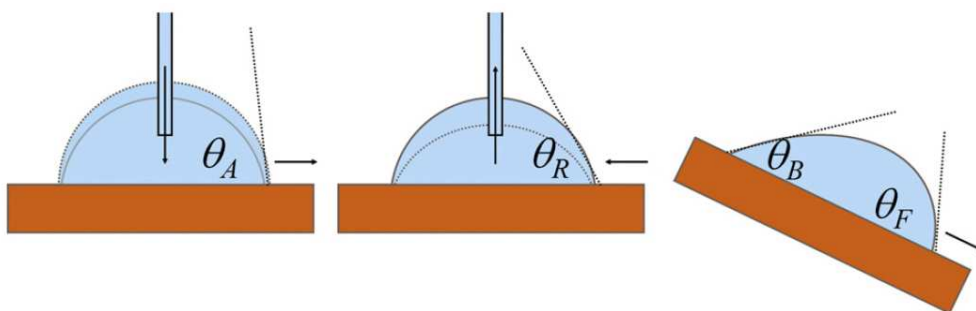

Figure 18. Measuring Advancing, receding and sliding angles.

In particular, for a sliding droplet the angles are influenced by its size. This means that results from different methods do not always agree and the method used to estimate droplet mobility or contact angle hysteresis should always be reported. The angle that a plate must be tilted to get a

droplet to slide depends upon the size of the drop and the difference between the cosines of the advancing and receding angles [48]. This angle can be easier to measure than the angles themselves and can be useful, as it describes the observable differences between surfaces. However, the strong dependence upon droplet volume and sensitivity to vibration can make it difficult to compare results between laboratories.

Some flat surfaces have very low contact angle hysteresis and, a clean piece of glass (only possible in a laboratory) can have a contact angle of 0° so must have no hysteresis. This means that any water reaching the surface forms a film and then drains off easily, droplets are never formed. This does mean that care must be taken when describing surfaces to provide both contact angle and hysteresis information. A low contact angle surface can be a surface that more easily sheds a liquid than a high contact angle one depending on the relative magnitudes of their contact angle hysteresis.

2.3.1 Superhydrophobicity and contact angle hysteresis

Experimentally it has been observed that hysteresis increases for a Wenzel surface and decreases for a surface with bridging type Cassie Baxter wetting. There are a few models that have been proposed to explain this [49, 50, 51].

In the 2D force diagram of a rough surface a drop in the Wenzel state can become pinned by the corners of roughness. However one would expect that the hysteresis of a bridging drop would also increase as the drop must advance round the corner of the pillar to jump to the next and it would recede at around the same angle as on a flat surface.

In 3D this is more complex because the contact line sits on a combination of pillars and holes at any time, meaning that the contact angle must only locally go down to the receding value. It is difficult to rationalise this as a 2D model as the weightings will depend on geometry.

A simpler way to look at the situation is to consider a surface to have intrinsic advancing and receding angles and to average out effects under the contact line by using the surface energy approach used earlier and therefore the Cassie-Baxter and Wenzel equations. As described before, the amplification effect of the Wenzel state then increases the difference between these values and increases hysteresis while the attenuation effect of the Cassie-Baxter bridging state reduces the difference between the values and therefore the hysteresis [49].

There is evidence that defects, contact line perimeter and sharp points induce hysteresis [50, 51]. Indeed one of the main theories for the existence of hysteresis of any sort is the presence of areas of different contact angle within the surface of a sample caused by local slope or chemistry, suggesting that a perfect single crystal could have very low hysteresis. This does not, however, lead to simple conclusions about how to increase or decrease hysteresis on a rough surface. As an example, McCarthy *et al* [52] showed that posts with different shapes but similar areas showed different hysteresis depending upon their shape with star shapes increasing hysteresis and circular pillars showing lower hysteresis. We showed that for circular pillars in a square lattice arrangement fabricated in SU-8, reducing the size and increasing the density to keep the global surface area fraction constant and therefore increasing the contact line perimeter had no discernible effect on the contact angle or hysteresis [42].

3. Methods for producing superhydrophobic surfaces

Generally a superhydrophobic surface only needs to be hydrophobic and rough on a scale much less than the capillary length (<273 µm for water). This leaves a huge scope for the actual chemistry and topography, and for topology. Additional constraints can be added to improve the properties of the material such as:

- Low solid surface fraction will improve sliding or rolling
- Tall, sharp, features increase the chance of inducing a bridging state, but weaken the surface against abrasion
- Pillars tend to form more "slippy" surfaces than holes, but are again weaker against abrasion
- Multiple length scales improve the effect, higher contact angles and more stable superhydrophobicity are produced than with a single scale roughness
- But a single, small, length scale considerably less than the wavelength of visible light is good for optical transparency
- The base material can be chosen for its properties and then coated to render it hydrophobic if necessary

A recent review focused on materials methods can be found in *Soft Matter* [53].

3.1. Textiles and fibres

Some of the first artificial superhydrophobic surfaces were textiles. Woven and non-woven fibrous materials possess high roughness and fibres lying horizontally have an undercut topography ideal for converting to superhydrophobicity and sometimes oleophobicity. Natural fibres are of the order of micrometers and artificial ones can be made much smaller, the fibres themselves can be roughened to enhance the effect. Some research has been carried out on improving the roughness and hydrophobicity of woven textiles to generate a stronger effect and non-woven mats of electrospun fibres have been found to be highly effective superhydrophobic surfaces and can be produced with very small fibre diameters.[54, 55, 56, 57]

3.2. Lithography

The two methods mostly used to produce superhydrophobic surfaces are photolithography, where a layer is illuminated through a patterned mask to activate areas and soft lithography, which is the small scale version of contact printing. A relatively high cost method that produces well-defined surfaces and can make many copies of the same thing. These have mostly been used to investigate the theories of wetting and in layered designs, such as microfluidics and electrowetting on complex electrodes. The advantage for theorists is that the r and f_s values of patterns and their symmetry can be varied to investigate the effects of these changes on the physical properties of the surfaces. The other advantage of photolithography is that it is a standard micro-engineering process that can easily be integrated into device fabrication [58, 59, 60, 61, 62,42].

3.3. Particles

Colloidal particles are often used to generate the roughness as they can be prepared in large amounts and can self arrange or form random surfaces. Superhydrophobic products, such as paint, are usually supplied in the form of particles in a binder that can be applied to a surface and allowed to set. More organised structures can be formed if the particles are aggregated under control and multiple particle sizes can be used to improve the effect. Several products are on the market that consist of particles suspended in a dilute matrix to produce a superhydrophobic paint [63, 64, 65].

3.4. Templating

A copy of any rough surface can be made by filling it with a soft or liquid material, hardening it and removing the original. This can be used to copy large areas of structure and has been used to make superhydrophobic surfaces by copying natural surfaces, such as leaves and insect wings and

originals made by the other techniques mentioned here. The advantage is that the original can often be reused and that the material of the copy can be chosen to a certain extent [66, 67, 68, 69, 70].

3.5. Phase separation

When a mixture begins to separate into its components it often forms an intermediate structure where the two phases interpenetrate. These structures can be frozen out if one of the separating phases solidifies before separation is complete. The structure can then be converted into a porous solid by removing one phase. This method has been used for some time to generate filters and stationary phases for chromatography, it is also very effective for generating superhydrophobic structures as the solid material is stable, overhangs and is often a polymer so can be hydrophobic on its own right. The size of the roughness can be varied by varying the system parameters and large surfaces can be prepared [71,72,73, 74].

3.6. Etching

Etching often increases the roughness of a surface and can be used to generate superhydrophobic surfaces. Any type of etching that increases roughness can be used, including acid etching of metals, plasma etching of polymers and laser etching of inorganic materials. Many combinations are possible and the technique is often combined with another roughness generation method to create multiple roughness scales [75, 76, 77, 78].

3.7. Crystal growth

The growth of crystals can generate rough surfaces, particularly if needle-like crystals can be produced. Nano-fibres can also be grown on surfaces using catalyst particles to direct growth. This produces surfaces with very high roughness and small size, important for the investigation of some extreme effects [79, 80, 81, 82].

3.8. Diffusion limited growth

This is the natural growth pattern when deposition occurs with no surface transport. It can occur in electrochemical growth and in gas phase deposition. The usual deposit looks much like a cauliflower head and has a fractal morphology with a very high surface area. Such surfaces are cheap to make on relatively small scale and can be made in a variety of materials [83, 84, 85, 86].

A selection of superhydrophobic surfaces are shown in Figure 19, showing the diversity in form that the roughness can take.
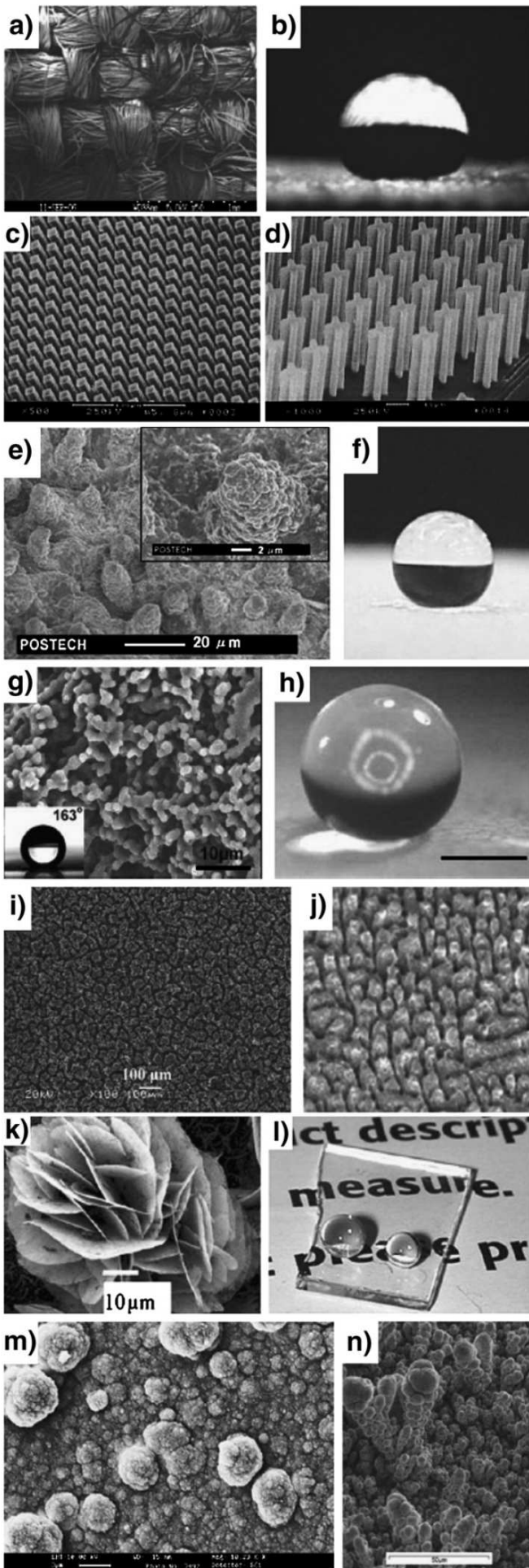
Figure 19. Superhydrophobic surfaces prepared in different ways, highlighting the various topographies possible a), b), textile superhydrophobic surfaces; c), d) Lithographic patterns; e), f) Templating; g) h), phase separation; i) j), Etching; k), l), crystal growth; m), n) diffusion limited growth. Reproduced with permission from. a) and b), Michielsen and Lee [54], c) and d) Oner and McCarthy [58], e) Lee and Kwon [69], f), Bormashenko et al. [70], g), Han et al. [73], h)Yamanaka et al. [74], i) Guo et al. [75], j) Baldacchini et al. [76], k), A. C. Chen, X. S. Peng, K. Koczkur, B.Miller, Chem. Commun., 2004, 17, 1964–1965, l), T. Ishizaki, N. Saito, Y. Inoue, M. Bekke, O. Takai, J. Phys. D., 2007, 40, 1, 192–197, m), Satyaprasad et al. [83], n) Shirtcliffe et al. [30]. Copyrights a, b, c, d, f, g, j, n, American Chemical Society, e, l, Institute of Physics, h, k, Royal Society of Chemistry, i, m, Elsevier.

4. Beyond simple hydrophobicity

4.1. Leidenfrost effect

The ideal superhydrophobic surface would be one whereby the solid surface fraction vanished (i.e. f_s=0). Whilst this may seem impractical to construct, it is known that when a droplet is placed on a surface at the Leidenfrost temperature, a temperature well above the boiling point of the liquid, a boundary layer of vapour be created. [87, 88] The layer of vapour reduces the heat transfer from the substrate and the rate of evaporation of the droplet is low, thus allowing it to persist. In this state, the droplet slides freely across the surface (Figure 20). This is effectively a Cassie-Baxter surface where the solid-surface fraction is zero, making the contact angle very high and the "slippyness" of the surface extremely high [89]. Similarly reduced evaporation has also been observed on superhydrophobic surfaces when the interfacial contact area determines the transfer of heat to the drop [90].

Figure 20. Leidenfrost drop; water on a heated surface. Reproduced with permission from Biance *et al.* [89]. Copyright American Institute of Physics 2003.

4.2. Super water repellent soil

Sand is a rough material, often with a grain size smaller than the capillary length of water. Under some conditions the surface of the grains can become hydrophobic and then the sand becomes repellent to water. This usually requires the presence of hydrophobic compounds coating the soil grains; these can be produced by plants, generated in a fire or spilled by man [31, 32].

If the grains are adhered to a surface the behaviour is much like that of a superhydrophobic surface, which is a problem because water does not penetrate very well and plants cannot grow as a result. In extreme cases water just persists on the surface, eventually evaporating or building into a flood. In most cases soaking the soil for a long period allows water to penetrate. Once the pores are filled with water the alternative Cassie-Baxter state is reached where the contact angle is reduced. If the soil dries it often reverts to superhydrophobicity. The problem is often remedied by adding surfactants to wet the soil or by adding a high surface area material such as clay to mop up the repellent chemicals.

4.3. Liquid marbles

If the grains are not fixed they adhere to the water droplet and eventually coat it; they are unlikely to escape unless their contact angle is very low or extremely high. In this way even PTFE spheres adhere strongly to the surface of water. The coated drop can then be moved onto a flat surface and will roll around on it as if the surface were superhydrophobic (Figure 21). Water liquid marbles with highly hydrophobic particles can even be placed onto water, where they will sit as

long as they are undisturbed, but will merge with the water below if pricked. The situation can be likened to a superhydrophobic surface where the roughness is attached to the droplet [91, 92, 93, 94],

Work on liquid marbles shows that these coated droplets bounce off flat surfaces and roll rapidly downhill. They barely interact with the surface, allowing them to behave like a soft solid. Their evaporation is much reduced as much of the air-liquid interface is replaced with solid-liquid interface.

Figure 21. A liquid marble of water with hydrophobised lycopodium powder rolling across a Petri dish.

4.4 Plastron respiration

One of the methods insects and arachnids, such as the spider in figure 1, use to breathe underwater is to carry a layer of air inside a superhydrophobic surface on their bodies and to breathe the gas in this layer. This layer, known as a plastron, differs from a bubble in that it cannot shrink, because the gas-water interface is maintained through capillary forces on a superhydrophobic structure. In a plastron, oxygen and carbon dioxide are continually exchanged between the film of air and the surrounding water. [95, 96, 97] Indeed some insects can remain underwater indefinitely because the air layer is continually replenished with oxygen. As the gas dissolves into the water an inwardly curved interface is produced. This supports a pressure difference so that the partial pressures of gases in the gas phase can be lower than those in the water thus causing a diffusion of gases across the gas-water interface. In contrast, a simple bubble always has an outwardly curved interface, ensuring that the gas in the bubble will eventually dissolve into the water. We have tested this by placing a fuel cell inside a superhydrophobic block and immersing it in oxygenated water [96]. Although the partial pressure of oxygen dropped it reached a constant value, effectively making an external gill (Figure 22).
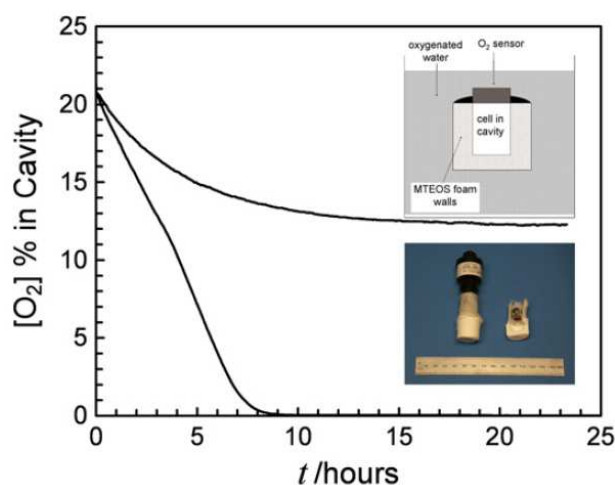

Figure 22. An artificial plastron constructed from a porous, superhydrophobic material; a fuel cell uses up the oxygen in the cavity and in an equivalent solid walled cavity showing the level of oxygen reaches a steady state as it diffuses in from the water into the gas phase. Reproduced with permission from Shirtcliffe *et al.* [96]. Copyright American Institute of Physics 2006.

4.5. Digital switching

As shown in figure 14 superhydrophobicity acts like an amplifier of contact angle. If the roughness of a surface is extreme enough the amplification effect will become very sharp and a small change in conditions will then cause a switch from non-wetting to fully wetting [11]. This principle is similar to that used in many detection devices and would allow a simple visual test. A suitable type of surface for this is a material with porous-type structure as the effective roughness can be very large.

In figure 23 a porous-structure hydrophobic material is heated to cause a small decrease in hydrophobicity (intrinsic contact angle), which causes a change from superhydrophobicity to wicking [22, 98].
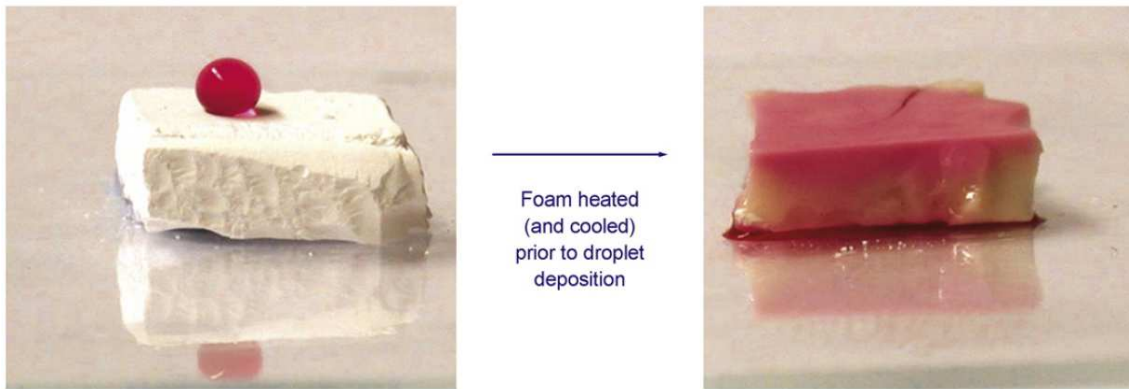

Figure 23. A porous foam is superhydrophobic. Heat treatment reduces its flat contact angle by a few degrees, but the extremely high roughness causes the material to switch to absorbing the liquid. Reproduced with permission from Shirtcliffe *et al.* [22]. Copyright Royal Society of Chemistry 2005.

4.6. Superspreading

As mentioned earlier in this article, a droplet wetting a rough surface will often exhibit a zero contact angle, but the rate at which it approaches this state is different to that on a flat surface with a zero contact angle. A droplet on a surface spreads until its contact angle, θ, reaches a stable value. On a smooth and flat surface, the driving force, F_d, for this is the out-of-balance component of the capillary force parallel to the surface,

$$F_d \propto \gamma_{LV}\left(\cos\theta_e - \cos\theta\right) \tag{12}$$

When the dynamic contact angle is small, the driving force can be approximated by,

$$F_d \propto \gamma_{LV}\left(\theta^2 - \theta_e^2\right) \tag{13}$$

In most cases the largest opposing force is viscous dissipation, which can be calculated for a liquid wedge shape assuming the wedge moves forward due to Poiseuille flow and a no-slip boundary condition is obeyed as the liquid-solid interface [99]. This results in dissipation inversely proportional to the tangent of the wedge angle. If the angle is small this is equivalent to being proportional to inverse θ. The edge speed (i.e. rate of change of contact radius), v_E, is then given by,

$$v_E \propto \gamma_{LV}\theta\left(\theta^2 - \theta_e^2\right) \tag{14}$$

which is the Hoffmann-Tanner-de Gennes law [100, 101, 99]. In the limit of a complete wetting surface (i.e. $\theta_e=0°$) the edge speed varies with the cube of the dynamic contact angle.

The driving force for spreading is changed for a droplet spreading in the Wenzel mode on a rough surface due to the increased surface area for interaction [102]. On a rough surface a wetting liquid will be in Wenzel mode so the equation becomes modified to

$$F_d \propto \gamma_{LV}\left(r\cos\theta_e - \cos\theta\right) \tag{15}$$

In this case, the constant terms in the small angle expansions of the cosines do not cancel, which means that the edge speed has both linear and cubic dependencies,

$$v_E \propto \gamma_{LV}\theta\left[(r-1)+\frac{1}{2}\left(\theta^2 - \theta_e^2\right)\right] \tag{16}$$

This also means that the edge speed will not slow as rapidly with decreasing contact angle as in the flat case and information about the surface roughness is encoded into the rate of spreading.

Spreading experiments using droplets of non-volatile polydimethylsiloxane (PDMS) on pillar surfaces with $\theta_e=0°$ have been used to examine equation 16 [102]. In the initial stages of spreading droplet volume was approximately maintained and the spreading droplet engulfed successive pillars. In later stages of spreading a film spread between pillars in advance of the droplet. The initial stages of spreading demonstrated a stick-slip pattern reflecting the pillar structure and an average slope consistent with a power law for $v_E \propto \theta^p$ with p between 1 and 3. When a series of patterns of increasing height were treated in the same manner the exponent changed from 3 down towards 1 as the height increased (Figure 24).
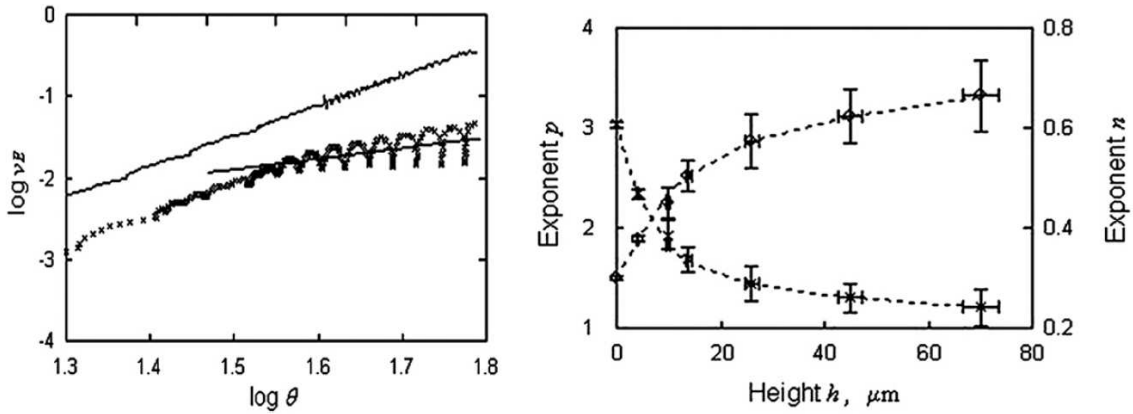

Figure 24. Left: a comparison of with log(edge speed) against log (contact angle) between a rough surface (lower curve) and a smooth one (upper curve) showing the rough surface has a region similar to the flat surface and one that is different. Right: The change in fitted exponent as the pattern is gradually increased in aspect ratio; exponent p changes from 3 towards 1, the change from a cubic towards a linear law, equally the exponent n linking contact angle and time changes from 0.3 towards 0.75. Reproduced with permission from McHale *et al.* [38]. Copyright American Physical Society.

4.7. Wetting and hemiwicking

In the previous section, the theory assumed that a droplet spread, but always upon a dry surface. Another possibility is that a liquid is imbibed by a surface pattern, spreading within the structure, but leaving the tops of the surface features dry. This is what happens after the initial spreading in the previous section. This situation has been called hemiwicking and has been

described by Quéré *et al.* among others [103, 104]. In droplet experiments, a wetting film can sometimes be seen to break away from the droplet and spread within the surface structure, generating a fried egg type pattern. As the liquid spreads within the surface structure, facets can be generated and its rate of spreading in different symmetry directions can be different. The shape of the wetted area may evolve with time as different facets advance at different rates. Figure 25 shows the development of facets that grow and merge like crystal planes as the wetting front escapes the drop edge [105].
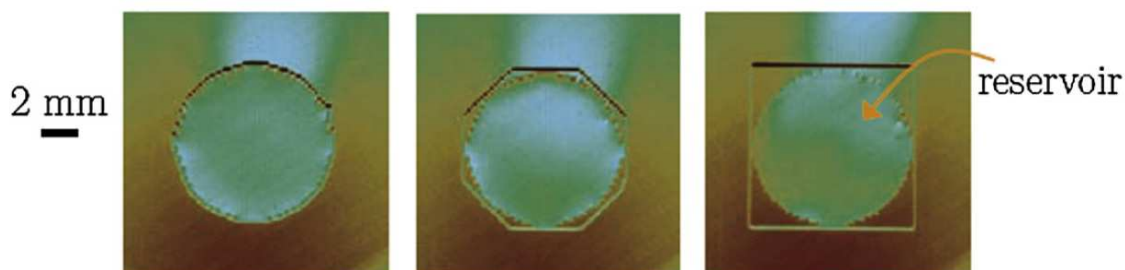

Figure 25. The progression of a drop from a circle to a square on the top of a square array of pillars. Reproducedwith permission from Courbin *et al.* [105]. Copyright American Physical Society 2007.

5. Summary and Conclusions

Superhydrophobicity in its simplest form is reasonably well understood and most surfaces follow some combination of Wenzel and Cassie-Baxter's equations, which can be understood as solutions for surface free energy minima that can have an energy barrier between them. Contact angle hysteresis is an important property of surfaces and how liquids move on them and is not directly linked with contact angle. For liquid shedding purposes a low contact angle hysteresis is more important than a high contact angle; fortunately Cassie-Baxter bridging superhydrophobic surfaces can provide both. When using these equations it is important to remember the principles upon which they are based and the assumptions used and which therefore define their validity. In many cases surfaces will not simply follow one or the other and it is often difficult to measure enough properties of the surfaces to allow combinations of the two equations to be used. The method by which liquids are deposited or condensed onto the surfaces can have a significant influence on the observed state. The increased interaction area of the Wenzel penetrating state and decreased interaction area of the Cassie bridging state can manifest themselves as amplification and attenuation of wetting and in the contact angle hysteresis and liquid spreading.

The shape of the topography and how many scales that it is rough over as well as the geometrical roughness and the contact angle of the chosen liquid on the chosen material all affect wetting and de-wetting. Wenzel's equation predicts that contact angles below 90° can be decreased by roughness and higher angles are increased, but the effect of bridging allows some surfaces with lower intrinsic contact angles to show increases in contact angle with roughness. The shape of the roughness is critical here to induce bridging. These factors allow extensive scope when designing a material for a particular purpose. Many methods can be used to generate superhydrophobic surfaces. All that are needed are sufficiently high intrinsic contact angle and surface roughness (or topography).

Many systems not considered before to be linked can be interpreted as a form of superhydrophobicity; soil hydrophobicity, insect plastron breathing and liquid marbles are some examples. Superhydrophobicity is one example of how topography interacts with surface chemistry to alter wetting properties. However, with a surface chemistry favouring wetting, topography also has an important interaction leading to superspreading, superwetting and other effects on rough surfaces.

There has been considerable research both recent and less recent into different aspects of superhydrophobicity and the areas are gradually being linked. Theory has advanced somewhat and more complicated aspects can often be simulated. A few applications have emerged, but superhydrophobic surfaces tend to make other liquids spread on them and the high aspect ratio roughness is fragile and easily damaged. The more successful applications lie so far in surfaces that do not encounter much oil or abrasion.

References

[1] Adamson, A. W., Gast, A. P.: Physical Chemistry of Surfaces. Wiley Blackwell: 1997.

[2] Denny, M. W.: Air and Water: The Biology and Physics of Life's Media. Princeton University Press: 1993.

[3] Turner, J. S.: The Extended Organism: The Physiology of Animal-Built Structures. Harvard University Press: 2000.

[4] de Gennes, P. G., Rev. Mod. Phys., 1985; **57** :827.

[5] Léger, L., Joanny J. F., Rep. Prog. Phys., 1992 ; **55** : 431.

[6] McHale G., Käb N. A., Newton M. I., Rowan S. M., J. Coll. Int. Sci., 1997; **186**: 453.

[7] Barthlott W., Neinhuis C., Planta, 1997; **202**: 1.

[8] Neinhuis C., Barthlott W.,: Ann. Bot., 1997; 79: 667

[9] Gao L., McCarthy T.J., Langmuir, 2008; 24: 9183.

[10] McHale G., Langmuir, 2009; 25: 7185.

[11] McHale G., Shirtcliffe NJ, Newton MI, Analyst, 2004; 129: 284.

[12] de Gennes PG, Brochard-Wyart F, Quéré D: Capillarity and Wetting Phenomena: Drops, Bubbles, Pearls, Waves. Springer: 2003.

[13] Quéré D, Annu. Rev. Mater. Res., 2008; 38:71.

[14] Gao LC, McCarthy TJ, Langmuir, 2007; 23: 3762.

[15] McHale G, Langmuir, 2007; 23: 8200.

[16] Wenzel RN, Ind. Eng. Chem., 1936; 28: 988.

[17] Wenzel RN, J. Phys. Colloid Chem., 1949; 53: 1466.

[18] Cassie ABD, Baxter S, Trans. Faraday Soc., 1944; 40: 546.

[19] Cassie ABD, Discuss. Faraday Soc., 1948; 3:11.

[20] Johnson RE, Dettre RH. In Gould RF (editor) Contact Angle, Wettability and Adhesion: Advances in Chemistry Series, Vol. 43, Am. Chem. Soc.: 1964. pp. 112–35.

[21] Bico J, Thiele U, Quéré D, Colloids Surf. A 2002; 206:41.

[22] Shirtcliffe N, McHale G, Newton M, Perry C, Roach P, *Chem. Commun*., 2005; (25): 3135.

[23] Quéré D, Nature Mater., 2002; 1:14.

[24] Patankar N, Langmuir, 2004; 20: 7097.

[25] Reyssat M, Yeomans J, Quéré D, Europhys. Lett., 81: art. 26006, (2008).

[26] Kusumaatmaja H, Blow M, Dupuis A, Yeomans JM, Europhys. Lett., (2008); 81: art. 36003.

[27] G. McHale, S. J. Elliott, M. I. Newton and N. J. Shirtcliffe, Superhydrophobicity: Localized parameters and gradient surfaces, in Mittal, K.L., ed, 'Contact Angle, Wettability and Adhesion', Koninklijke Brill NV, Vol. 6, 219-233 (2009).

[28] Shastry A, Case MJ, Böhringer KF, Langmuir, 2006; 22: 6161.

[29] Sun, Zhao XW, Han YH, Gu ZZ, Thin Solid Films, 2008; 516: 4059.

[30] Shirtcliffe N, McHale G, Newton M, Perry C, Langmuir, 21: 3, 937-943, (2005)

[31] McHale G, Newton MI, Shirtcliffe NJ, Eur. J. Soil Sci., 2005; 56: 445.

[32] Bachmann J, McHale G, Eur. J. Soil Sci., 2009; 60: 420.

[33] Tuteja A, Choi W, Ma ML, Mabry JM, Mazzella SA, Rutledge GC, McKinley GH, Cohen RE, *Science*, 2007; 318: 1618.

[34] M. Nosonovsky, *Langmuir*, 2007, **23(6)**, 3157-3161

[35] C. H. Chen, Q. J. Cai, C. L. Tsai, C. L. Chen, G. Y. Xiong, Y. Yu, Z. F. Ren, *Appl. Phys. Lett*.,2007, **90(17)**, 173108

[36] Shirtcliffe N, McHale G, Newton M, Chabrol G, Perry C, *Adv. Maters.*, 2004; 16: 1929.

[37] Patankar N., *Langmuir*, 20: 17, 7097-7102, (2004)

[38] McHale G, Shirtcliffe N, Aqil S, Perry C, Newton M, *Phys. Rev. Lett.*, 2004; 93: art. 036102

[39] Herminghaus, S., *Europhys. Lett.*, 52: 2, 165-170, (2000)

40   Tuteja, A., , Choi, W., Ma, M., Mabry, J., Mazzella, S., Rutledge, G., McKinley, G., Cohen, R., *Science*, 318: 5856, 1618-1622, (2007)

41   Patankar, N.A. *Langmuir*, <u>20</u> (2004) 8209-8213

42   Shirtcliffe N, Aqil S, Evans C, McHale G, Newton M, Perry C, Roach P, *J. Micromech. Microeng.*, 14: 10, 1384-1389, (2004)

43   Ishino C, Okumura K, Quere D, *Europhys. Lett.*, 68: 3, 419-425(2004)

44   Dorrer, C., Ruhe, J., *Langmuir*, 23: 7, 3820-3824, (2007).

45   Cheng YT, Rodak DE, Angelopoulos A, Gacek T., *Appl. Phys. Lett.*, 2005; 86: art. 194112.

46   Wier K, McCarthy T., *Langmuir*, 2006; 22: 2433.

47   Krasovitski B, Marmur A, *Langmuir*, 21: 9, 3881-3885, (2005)

48   Miwa M, Nakajima A, Fujishima A, Hashimoto K, Watanabe T, *Langmuir*, 2000; 16: 5754.

49   McHale G, Shirtcliffe N, Newton M., *Langmuir*, 20: 10146, (2004).

50   Gao LC, McCarthy TJ, *Langmuir*, 22: 6234, (2006).

51   Reyssat M, Quéré D, J. Phys. Chem. B, 2009; 113: 3906.

52   Chen W, Fadeev A, Hsieh M, Oner D, Youngblood J, McCarthy T., *Langmuir*, 15: 10, 3395-3399, (1999)

53   Roach P, Shirtcliffe, N J and Newton M I, *Soft Matter* 4, 224, (2008).

54   S. Michielsen, H. J. Lee, *Langmuir*, 2007, **23, 11**, 6004-6010

55   Y. Y. Liu, R. H. Wang, H. F. Lu, L. Li, Y. Y. Kong, K. H. Qi, J. H. Xin, *J.Mater. Chem.*, 2007, **17, 11**, 1071-1078

56   T. Wang, X. Hu, S. Dong, *Chem. Commun.*, 2007, 1849-1851

57   M. Ma, M. Gupta, Z. Li, L. Zhai, K. K. Gleason, R. E. Cohen, *Adv Materials.*, 2007, **19**, 255-259

58   D. Oner, T. J. McCarthy, *Langmuir*, 2000, **16, 20**, 7777-7782

59   Z. Yoshimitsu, A. Nakajima, T. Watanabe, K. Hashimoto, *Langmuir*, 2002, **18, 15**, 5818-5822

60   L. Zhu, Y. Y. Feng, X. Y. Ye, Z. Y. Zhou, *Sens. Act. A.*, 2006, **130**, 595-600

61   C. H. Choi, C. J. Kim, *Nanotechnology*, 2006, **17, 21**, 5326-5333

62   R. M. Wagterveld, C. W. J. Berendsen, S. Bouaidat, J. Jonsmann, *Langmuir*, 2006, **22, 26**, 10904-10908

63   Y. Li, X. J. Huang, S. H. Heo, C. C. Li, Y. K. Choi, W. P. Cai, S. O. Cho, *Langmuir*, 2007, **23(4)**, 2169-2174

64   C. Sun, L. Q. Ge, Z. Z. Gu, *Thin Solid Films*, 2007, **515, 11**, 4686-4690

65   Patents, e.g CN1919938 (A) and US2004081818 (A1)

66   J. Bico, C. Marzolin, D. Quere, *Europhys. Lett.*, 1999, **47, 2**, 220-226

67   R. A. Singh, E. S. Yoon, H. J. Kim, J. Kim, H. E. Jeong, K. Y. Suh,, *Mater. Sci. Eng. C.*, 2007, **27, 4**, 875-879

68   J. Li, J. Fu, Y. Cong, Y. Wu, L. J. Xue, Y. C. Han, *Appl. Surf. Sci.*, 2006, **252(6)**, 2229-2234

69   S-M. Lee, T. H. Kwon, *J. Micromech. Microeng.*, 2007, **17**, 687-692

70   E. Bormashenko, T. Stein, G. Whyman, Y. Bormashenko, R. Pogreb, *Langmuir*, 2006, **22, 24**, 9982-9985

71   N. J. Shirtcliffe, G. McHale, M. I. Newton, C. C. Perry, P. Roach, *Mater. Chem. Phys.*, 2007, 103, 1, 112-117

72   X. Li, G. Chen, Y. Ma, L. Feng, H. Zhao, *Polymer*, 2006, **47**, 506-509

73   J. T. Han, X. R. Xu, K. W. Cho, *Langmuir*, **21 (15)**, 2005, 6662-6665

74   M. Yamanaka, K. Sada, M. Miyata, K. Hanabusa, K. Nakano, *Chem Commun.*, 2006, **21**, 2248-2250

75   Z. Guo, F. Zhou, J. Hao, W. Liu, *J. Colloid Int. Sci.*, 2006, **303**, 298-305

76   T. Baldacchini, J. E. Carey, M. Zhou, E. Mazur, *Langmuir*, 2006, **22**, 4917-4919

77   L. M. Lacroix, M. Lejeune, L. Ceriotti, M. Kormunda, T. Meziani, P. Colpo, F. Rossi, *Surf. Sci.*, **592(1-3)**, 182-188, (2005)

78   Lacroix LM, Lejeune M, Ceriotti L, Kormunda M, Meziani T, Colpo P, Rossi F, Surf. Sci., 592 (1-3): 182-188, (2005)

79   Onda T, Shibuichi S, Satoh N and Tsujii K, 1996 Langmuir 12 2125.

80   X. D. Wu, L. J. Zheng, D. Wu, *Langmuir*, 2005, 21, 2665-2667

81   K. K. S. Lau, J. Bico, K. B. K. Teo, M. Chhowalla, G. A. J. Amaratunga, W. I. Milne, G. H. McKinley, and K. K. Gleason, *Nano Lett.*, 2003, **3**, 1701-1705

82   H. Liu, L. Jiang, *Soft Matter*, 2006, **2**, 811-21

83   A. Satyaprasad, V. Jain, S. K. Nema, *Appl. Surf. Sci.*, 2007, **253, 12**, 5462-5466

84   N. J. Shirtcliffe, G. McHale, M. I. Newton, C. C. Perry, *Langmuir*, 2005, **21(3)**, 937-943

85   S. Karuppuchamy, J. M. Jeong, *Mater. Chem. Phys.*, 2005, **93**, 251-254

[86] N. J. Shirtcliffe, P. Thiemann, M. Stratmann, G. Grundmeier, *Surf. Coatings Tech.*, 2001, **142**: 1121-1128

[87] Leidenfrost J., *De Aquae Communis Nonnullis Qualitatibus Tractatus* 1756

[88] Gottfried B., Internat. J. Heat Mass Transfer 9 : 1167, (1966)

[89] Biance A, Clanet C, Quéré D, Phys. Fluids., 2003; 15: 1632

[90] Takata Y, Proc. 4th International Conference on Nanochannels, Microchannnels, and Minichannels, Pts A and B, 1333-1341, (2006)

[91] Aussillous P, Quere D Nature, 411: 6840, 924-927(2001)

[92] Dorvee J, Derfus A, Bhatia S, Sailor M, Nature Mater., 3: 12, 896-899, (2004)

[93] McHale, G., Shirtcliffe N, Newton M, Pyatt F, Doerr S, Appl. Phys. Lett., 90: 5, 054110, (2007)

[94] Pike N, Richard D, Foster W, Mahadevan L, Proc. Royal Soc. London B, 269: 1497, 1211-1215, (2002)

[95] Thorpe, W.H. Biol. Rev. 1950, 25, 344-390.

[96] Shirtcliffe N, McHale G, Newton, M, Perry C., Pyatt F. Appl. Phys. Lett. 89 (2006) art. 104106.

[97] Bush J, Hu D, Prakash M, Adv. Ins. Physiol. 34 (2008) 117-192

[98] Shirtcliffe N, McHale G, Newton M, Perry C, Roach P, Maters. Chem. Phys., 2007; 103: 112.

[99] P.G. De Gennes, *Rev. Mod. Phys.* **57** (1985), p. 827.

[100] R.A. Hoffman, *J. Colloid Interface Sci.* **50** (1975), p228.

[101] L.H. Tanner, *J. Phys. D* **12** (1978), p. 1473.

[102] McHale G, Shirtcliffe N, Aqil S, Perry C, Newton M, Phys. Rev. Lett., 93: 3, 036102, (2004)

[103] Ishino C, Reyssat M, Reyssat E, Okumura K, Quere D, Europhys. Lett., 79, 5, 56005, (2007)

[104] Starov V, Zhdanov S, Kosvintsev S, Sobolev V, Velarde M, Adv. Coll. Interf. Sci., 104, 123-158, (2003)

[105] Courbin L, Denieul E, Dressaire E, Roper M, Ajdari A and Stone H A, 2007, Nat. Mater. 6 661.